1/f noise characteristics of waveguide-integrated PbTe MIR detectors and impact on limit of detection

Emanuele Guglielmi, Peter Su, Francesco Zanetto, Katherine Stoll, Samuel Serna, Giorgio Ferrari, *Member, IEEE*, Marco Sampietro, *Member, IEEE*, Kazumi Wada, Lionel C. Kimerling, Anuradha Agarwal

***Abstract*—The noise power spectral density of a detector is essential for determining the frequency of operation and readout architecture that yields an optimal signal-to-noise ratio. In this work, we characterize a waveguide-integrated PbTe mid-infrared detector and report on its noise spectrum, highlighting the presence of a current-dependent 1/f term dominating at low frequency and/or high bias over the Johnson component typical of a photoconductor. This behaviour, together with the substantially flat frequency response in the range between $1\,\mathrm{kHz}$ to $1\,\mathrm{MHz}$, guide towards a lock-in readout strategy, that allows one to operate in the region of minimum noise without penalties in the detection performance. Practical guidelines to optimize the readout resolution are provided and the limit of detection of a gas sensing system exploiting PbTe photoconductors is derived, as an example of how a careful co-design of sensors and electronics can dramatically improve the detection performance.**

***Index Terms*—integrated photonics, solid-state MIR detector, noise characterization, lock-in readout, gas sensing.**

I. Introduction

Binary lead chalcogenides like PbTe, PbSe and PbS have been demonstrated as suitable materials for room temperature mid-infrared (MIR) detectors [1, 2]. The deposition and processing of lead chalcogenide thin films play a huge role in the resulting material properties, while oxygen annealing and sensitization is important for achieving the desirable mid-infrared photodetecting properties [3]. PbS and PbSe detectors are produced commercially in film form using a chemical deposition technique [4, 5, 6, 7], so there are currently no commercially available detectors produced using evaporation methods, required for easy patterning and integration on chip. However, unlike PbS and PbSe, PbTe thin film photoconductors can be deposited onto any substrate by thermal evaporation [8, 9, 10] through a low temperature process that allows patterning via either a shadow mask or a lithography liftoff process. The low temperature also enables back-end Si-CMOS integration and direct deposition on read out integrated circuits (ROICs), avoiding adverse high temperature dopant diffusion in the underlying electronic circuits. PbTe films have successfully been used in waveguide-integrated detectors for on-chip gas sensors [11, 12], important for applications in industry, environment and homeland security. The well-known trend of Internet of Things (IoT) and the newer Internet of Everything (IoE) are expected to boost their use and lead to integrated, compact, low power consumption and connected solutions [13].

We have focused our research on a solid-state optoelectronic solution employing a PbTe mid-infrared waveguide-integrated detector. To achieve superior photodetection performance, the electrical properties of the detector and the electronic measuring architecture must be evaluated. We have fully characterized the PbTe detector in terms of responsivity to light, signal bandwidth and noise spectrum and derived an optimal measuring strategy in terms of operating frequency and modulation scheme to increase the signal-to-noise ratio (S/N) of the measurement. The paper describes in detail the noise spectrum analysis and finally reports its impact on the limit of detection (LOD) of a PbTe-based gas sensing solid-state optoelectronic system.

II. Optical and electrical characterization of the detector

The detectors characterized in this work are PbTe MIR photoconductors monolithically integrated on chalcogenide waveguides and fabricated following a process similar to that outlined in [12, 14]. On a silicon wafer with $3\,\mu\mathrm{m}$ thermal oxide, a $100\,\mathrm{nm}$ PbTe film was deposited via thermal evaporation and patterned using photolithography [15, 16]. As noted previously [15], PbTe films are stoichiometric, single face centered cubic (FCC) phase, polycrystalline films and exhibit (200) texture even on amorphous glass substrates. Band conduction model in the high temperature region yields an electrical band gap energy between $0.2\,\mathrm{eV}$ and $0.3\,\mathrm{eV}$ [17, 18, 19], smaller than the energy of MIR photons up to $4300\,\mathrm{nm}$ wavelength.

After the deposition of the PbTe film, a $300\,\mathrm{nm}$ layer of thermally evaporated Sn was used to ensure ohmic connection between the detector and the contact pads, made of a bilayer consisting of $80\,\mathrm{nm}$ Au with a $20\,\mathrm{nm}$ Ti adhesion layer. A

Manuscript received –; revised –. This work was supported by Progetto Rocca Foundation.

E. Guglielmi, F. Zanetto, G. Ferrari and M. Sampietro are with the Department of Electronics, Information and Bioengineering, Politecnico di Milano, 20133 Milano, Italy (e-mail: emanuele.guglielmi@polimi.it; francesco.zanetto@polimi.it; giorgio.ferrari@polimi.it; marco.sampietro@polimi.it).

P. Su, K. Stoll, S. Serna, K. Wada, L. C. Kimerling and A. Agarwal are with the Department of Materials Science & Engineering and Materials Processing Center, Massachusetts Institute of Technology, Cambridge, MA 02139 USA (e-mail: pxsu25@gmail.com; kestoll@mit.edu; safes@mit.edu; kwada@mit.edu; lckim@mit.edu; anu@mit.edu).

S. Serna is also with the Department of Physics and Photonics and Optical Engineering, Bridgewater State University, Bridgewater, MA 02324 USA

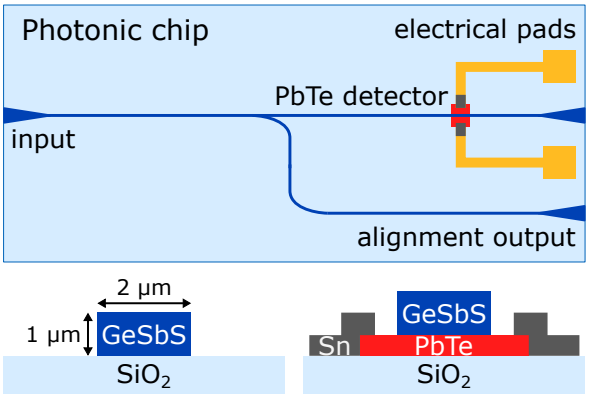

Fig. 1. Top view and cross sections of the photonic chip, with a glass chalcogenide waveguide and a PbTe detector integrated directly underneath it.

1 µm thick GeSbS waveguide was then deposited using thermal evaporation and patterned using electron beam lithography and liftoff. The wafer piece was finally cleaved to create input and output waveguide facets. A schematic of the chip is shown in Figure 1.

Figure 2 shows the optical and electronic parts of the fabricated device. The electrical pads displayed in Figure 1 are apparent in the photonic integrated chip.

A. Electrical characterization

Six PbTe photoconductors have been integrated on a single chip and electrically characterized to assess their effective resistance and linear behavior. The measurements, shown in Figure 3, confirm the excellent ohmic nature of the Sn to PbTe contacts, the good reproducibility of the fabrication process and the linear behavior for small voltage biases, with a detector resistance around 13 kΩ varying less than 1% when biased at 1 V. The measurements have been performed with a bench-top source-meter with the chip connected to a small PCB holder.

B. Optical response

The optical responsivity of the PbTe detector has been measured using a tunable laser set at 2361 nm, modulated with a mechanical chopper at 1 kHz and coupled into the chip

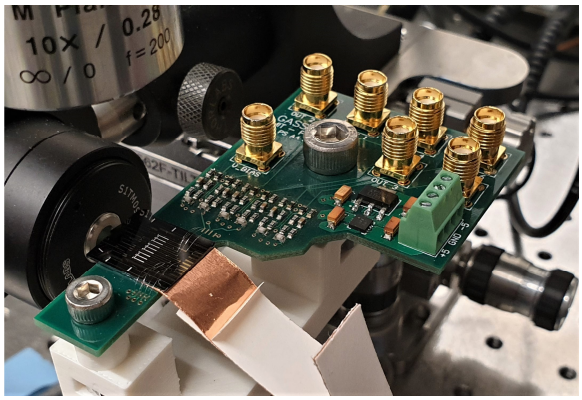

Fig. 2. Image of the electro-optical device.

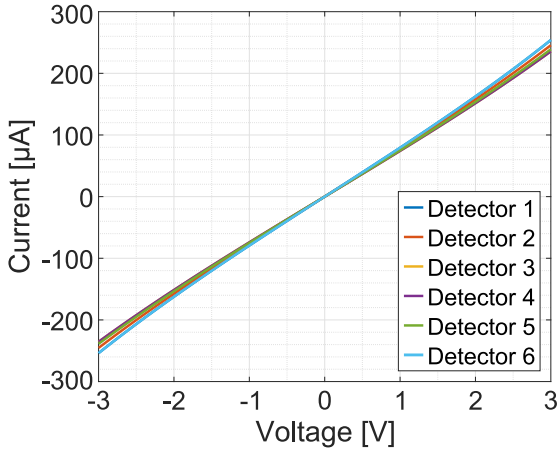

Fig. 3. Measured I-V curves of six detectors integrated on the same chip, highlighting the good ohmic contact of the Sn layer to the PbTe film and the reproducibility of the fabrication process.

with an aspheric lens (Figure 4). The light inside the chip is split by a 3 dB splitter: one of the two arms illuminates the integrated PbTe detector, while the other directly exits from the chip for alignment purposes. The detector was biased at 1 V and its signal was detected with a commercial transimpedance amplifier (TIA) and measured by a lock-in amplifier locked to the chopper frequency. The light power was varied with a neutral density filter in the beam path and measured at the input of the chip with a thermal power meter. Considering the coupling loss of about 5 dB at the chip facet and the 3 dB splitter, the measured responsivity to light of the integrated detector can be expressed in terms of variation of its conductance as:

$$\Delta G = \Delta G_0 \cdot \left(\frac{P_{OPT}}{1\,\mathrm{mW}} \right)^{\eta} \tag{1}$$

where P_{OPT} is the optical power that reaches the detector, $\Delta G_0 = 90\,\mathrm{nS}$ and $\eta = 0.816$. This expression has been derived by fitting the experimental curve of Figure 5a, that shows a slightly sub-linear behaviour. The current signal due to light, that is summed to a constant baseline due to the dark conductance of the detector, is then simply obtained as $I_{DET} = V_{BIAS} \cdot \Delta G$, where V_{BIAS} is the bias voltage.

The frequency response of the photoconductor could not be measured at the same 2361 nm wavelength because mechanical choppers can only generate modulations up to few kHz and electro-optical modulators in the mid-infrared region were not available to us. For this reason, the measurement has been performed with a 1 mW laser at 1550 nm with a user selectable square-wave modulation from 1 kHz to 1 MHz, taking advantage of the equally strong response of PbTe detectors at this telecom wavelength [20]. The signal from the PbTe detector was once again amplified with the same commercial TIA and detected with a lock-in amplifier, locked to the laser modulation frequency. The measured frequency response $R(f)$, normalized with respect to the signal at 1 kHz, is reported in Figure 5b. The PbTe detector shows a response with less than a factor of 2 reduction over three decades of

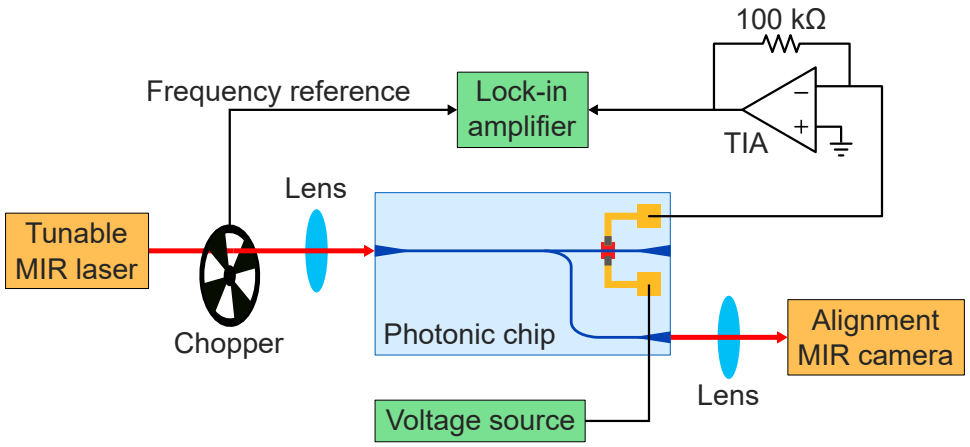

Fig. 4. Experimental setup used to characterize the optical response of the detector.

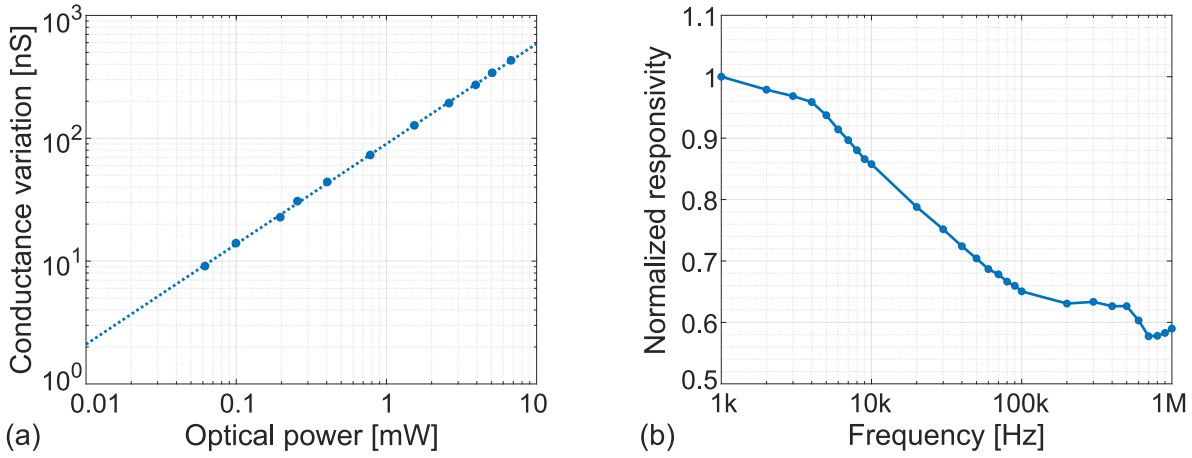

Fig. 5. (a) Responsivity curve of the PbTe detector biased at 1 V, measured at 2361 nm. (b) Frequency response of the detector biased at 1 V, measured with a 1 mW square-wave modulated laser at 1550 nm and normalized with respect to the signal at 1 kHz.

frequency, suggesting that it can be used to detect signals over a wide range of frequencies.

III. Noise Spectral Characterization

In addition to the optical characteristics and frequency response, an essential information often overlooked when designing and using integrated detectors is the noise behavior, that can determine their best operating conditions in terms of bias and readout frequency and the requirements of the electronics.

To perform the noise characterization of the PbTe detector, one of its terminals was connected to the virtual ground of the TIA, followed by an additional voltage amplifier to amplify the noise information above the input noise level of the spectrum analyzer being used to perform the measurement. The other contact was connected to a voltage generator, swept between 0 V and 5 V to operate the detector at different biases. The measurement was performed after enclosing the detector and the TIA into a grounded metallic container to shield the device from electromagnetic noise.

The acquired noise spectrum is shown in Figure 6a highlighting, in addition to the thermal contribution S_J, a strong term $S_{1/f}$ inversely proportional to the frequency, typical of a 1/f noise, that follows Hooge's Empirical Rule [21]:

$$S_I(f) = S_J + S_{1/f} = \frac{4kT}{R_{DET}} + k_H \frac{I^2}{f} = \\ = \frac{4kT}{R_{DET}} + k_H \frac{V_{BIAS}^2}{f \cdot R_{DET}^2} \left[\frac{\mathrm{A}^2}{\mathrm{Hz}}\right] \quad (2)$$

where R_{DET} is the detector resistance, I the current flowing through it, V_{BIAS} the bias voltage, f the frequency and k_H is a constant that was estimated around 3.52×10^{-10} in our case. When the bias of the detector is increased, the corresponding linear variation of the current (see Figure 3) causes a quadratic enhancement of the noise power spectral density as seen in Figure 6.

To disentangle the intrinsic noise contribution of the PbTe material from the instrument measuring limit, we compared the noise spectrum of the detector with that of a discrete resistor of equivalent value, for voltage biases of 0 V and 1 V. The results are shown in Figure 6b. The discrete resistor does not exhibit any current-dependent 1/f noise, showing that this term is indeed due to the intrinsic nature of the PbTe

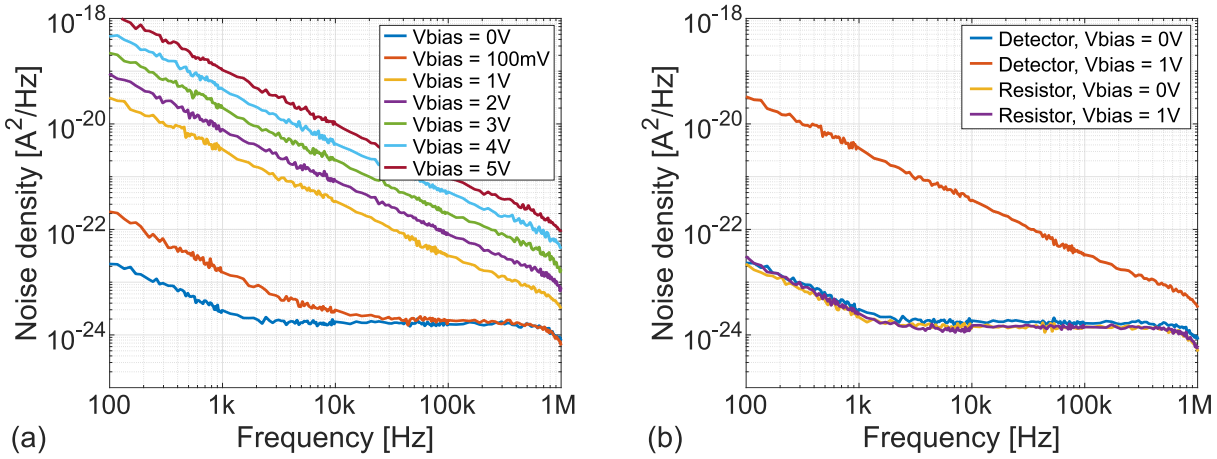

Fig. 6. (a) Current noise power spectral density of the integrated PbTe detectors for different bias voltages between 0 V and 5 V and (b) comparison with a discrete resistor of equivalent value.

material. Note that the PbTe detector, when biased at 0V (no current flowing, i.e. at thermodynamic equilibrium), shows the same white noise level as the discrete resistor, confirming that the Johnson noise is the dominant term at low bias or at high frequency. The residual 1/f noise measured at very low frequencies, being equal in both the discrete resistor and in the PbTe photoconductor at zero bias, is attributed to the measuring instrument.

The noise behaviour gives important guidelines to determine the optimal bias point of the detector. A high bias produces a large electrical signal ($I_{DET} = V_{BIAS} \cdot \Delta G$), but also a higher noise with the same dependence ($\sqrt{S_I(f)} \propto V_{BIAS}$). Increasing the bias of the detector thus does not offer any benefit in terms of SNR when the 1/f noise term dominates. The optimal bias point is identified with the voltage that moves the 1/f noise corner frequency (frequency at which the 1/f component is equal to the white noise) to the measuring frequency f_{AC}. Considering the parameters computed from the noise spectrum and assuming that the noise of the electronics is negligible, voltages of $80\,\mathrm{mV}$ and $250\,\mathrm{mV}$ are sufficient when operating at $10\,\mathrm{kHz}$ and $100\,\mathrm{kHz}$, respectively. Higher bias voltages would not improve the S/N any further.

A. Contribution to noise from materials properties

The origin of the 1/f noise that dominates at lower frequencies in PbTe films is not fully understood, but defects likely play a large role as a source of 1/f noise in these photoconductors due to their polycrystalline nature. While all semiconductors have some point defects within their bulk, polycrystalline films can also have defects as dangling bonds located at grain boundaries [22, 23, 24]. Although the exact location or nature of the defects in polycrystalline PbTe films has not yet been conclusively determined, oxygen has been shown to improve photoconductivity and could be passivating defects along the grain boundaries while making the grain boundaries more p-type [3]. Hence PbTe films are usually produced using two steps: evaporation of an approximately stoichiometric source onto a target substrate followed by an oxygen sensitization step [8, 9].

This sensitization and potential passivation by oxygen can occur at room temperature [20], but it is often done by annealing in oxygen ambient at higher temperatures (250 to 300 °C). However, to ensure back-end Si-CMOS integration, no high temperature annealing has been performed in this sample. Further investigation is needed to determine whether high temperature annealing has an impact on the passivation of defects and therefore on the noise of the PbTe photoconductor.

IV. Lock-in readout strategy and limit-of-detection assessment

The noise behaviour shows a 1/f component, while the responsivity spectrum remains substantially unchanged as the frequency increases. This guides the readout strategy of the sensor towards a lock-in architecture, and allows us to optimize the S/N of the measurement by selecting the operating frequency, f_{AC}, where the noise of the detector is lower. In this particular case, a higher modulation frequency allows us to increase the bias voltage of the photoconductor while still operating in the region of minimum noise, with a great advantage in terms of measurement sensitivity. The modulation of the light input signal can be obtained with an external chopper, with a modulated laser or with a monolithic modulator integrated with the chalcogenide waveguide, depending on the required operating frequency and available technology. Although modulating the detector bias achieves the same shift in frequency of the signal to be measured, this method is not effective in improving the S/N because it equally shifts the detector noise spectrum. The lock-in readout also allows one to choose the most suitable measurement time, i.e. detection bandwidth, to achieve the sensitivity/resolution required by the application, down to the limit given by the readout instrument or to the intrinsic fluctuations of the modulation signal [25].

To quantify the effect of proper lock-in detection on the measurement resolution, let us consider an example photonic chip where the chalcogenide spiral and the PbTe element are used to detect the presence of a particular gas species in the environment, as reported in [11, 12] and shown in Figure 7. The detection of gas is possible due to its interaction

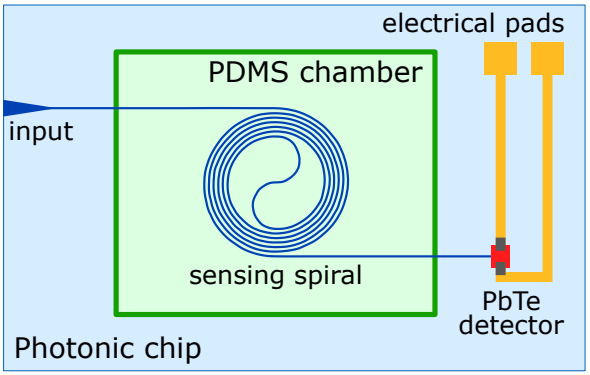

Fig. 7. Schematic of the gas sensing photonic chip integrating a spiral chalcogenide waveguide with a PbTe detector. The PDMS chamber is used to control the concentration of gas that interacts with the chip.

with the evanescent tail of light from the unclad waveguide. Gases like methane have distinct absorption peaks in the MIR range [26, 27, 28], so their presence can be detected by monitoring the amount of light transmitted through the waveguide at specific wavelengths. By using a spiral geometry, the interaction length between light and gas can be increased while keeping a compact form factor, an important advantage over bulky systems employing discrete optics. The minimum volume concentration of gas that can be detected by this architecture is determined both by the spiral length [29] and by the resolution in the readout of the PbTe photoconductor. In fact, the spiral length determines the interaction of light and gas as well as the propagation losses, while the readout noise determines the smallest electrical signal that can be measured. Both aspects need to be optimized to obtain the best detection performance.

According to Beer-Lambert Law, the transmittance of the waveguide and its dependence on gas concentration can be written as:

$$T = T_0 \cdot T_{GAS} = e^{-\beta \cdot L} \cdot e^{-\alpha \cdot \Gamma \cdot L \cdot C} \tag{3}$$

where β is the propagation loss of the waveguide, α the absorbance of pure gas at atmospheric pressure, Γ the confinement factor in the gas, L the spiral length and C the volume concentration [12]. Considering a modulated light source at f_{AC} and thus neglecting the DC dark current, the current signal of the PbTe detector I_{DET} is given by the responsivity of Equation 1, the frequency response of Figure 5b at f_{AC} and the current noise i_n:

$$\begin{aligned} I_{DET} &= V_{BIAS} \cdot \Delta G_0 \cdot \left(\frac{P_{OPT}}{1\,\mathrm{mW}}\right)^{\eta} \cdot R(f_{AC}) + i_n = \\ &= V_{BIAS} \cdot \Delta G_0 \cdot \left(\frac{P_{IN} \cdot T_0 \cdot T_{GAS}}{1\,\mathrm{mW}}\right)^{\eta} \cdot R(f_{AC}) + \\ &+ i_n = I_0 \cdot T_{GAS}^{\eta} + i_n \end{aligned} \tag{4}$$

where P_{IN} is the optical power at the input of the spiral-detector sequence and $I_0 = V_{BIAS} \cdot \Delta G_0 \cdot \left(\frac{P_{IN} \cdot T_0}{1\,\mathrm{mW}}\right)^{\eta} \cdot R(f_{AC})$ is the detector current in the absence of gas. In the expression we have neglected the intensity noise of the laser, significant only in case of large laser power instabilities. The baseline current signal I_0 with no gas ($T_{GAS} = 1$) reduces when the concentration of analyte increases ($T_{GAS} < 1$). The difference between the two currents needs to be compared to the RMS value of the photoconductor noise to determine the minimum volume concentration that can be detected, leading to the expression of the S/N of the measurement:

$$S/N = \frac{I_0 - I_0 \cdot T_{GAS}^{\eta}}{i_{n,RMS}} = \frac{I_0 \left(1 - T_{GAS}^{\eta}\right)}{\sqrt{S_I(f_{AC}) \cdot BW}} \tag{5}$$

where $S_I(f_{AC})$ is the detector current noise power spectral density measured at f_{AC} and BW is the lock-in readout bandwidth. By first deriving T_{GAS}^{η} from the S/N expression and then recalling its dependence on gas concentration (equation 3), it is possible to write:

$$e^{-\alpha \cdot \Gamma \cdot L \cdot LOD \cdot \eta} = 1 - \frac{S/N \cdot \sqrt{S_I(f_{AC}) \cdot BW}}{I_0} \tag{6}$$

where LOD is the limit of detection of the gas sensing system expressed in volume concentration. The LOD can finally be written as:

$$\begin{aligned} LOD = &-\frac{1}{\alpha \cdot \Gamma \cdot L \cdot \eta} \cdot \\ &\cdot \ln\left[1 - \frac{S/N \cdot \sqrt{S_I(f_{AC}) \cdot BW}}{V_{BIAS} \cdot \Delta G_0 \cdot \left(\frac{P_{IN} \cdot e^{-\beta \cdot L}}{1\,\mathrm{mW}}\right)^{\eta} \cdot R(f_{AC})}\right] \end{aligned} \tag{7}$$

The equation quantifies the interplay between the laser power, the spiral sensor characteristics and the detector behaviour. Notice that proper knowledge of the PbTe detector element and correct lock-in processing allow one to dramatically optimize the Limit of Detection (LOD). As long as the 1/f term of the detector noise is not dominant, V_{BIAS} can be increased, obtaining a relevant improvement in the measurement resolution. For the same reason, it is better to work at high frequency, as V_{BIAS} can be further increased while still operating in the region of minimum noise without significant trade-offs, given the flat frequency response of the photoconductor. Finally, the lock-in detection bandwidth can be arbitrarily set to obtain the desirable measurement resolution. Figure 8a shows the LOD computed as a function of the light modulation frequency in an example scenario of methane sensing, using the spiral parameters reported in [11] ($\alpha = 37.3\,\mathrm{cm}^{-1}$, $\Gamma = 0.125$, $L = 5\,\mathrm{cm}$, $\beta = 8\,\mathrm{dB\,cm}^{-1}$), $P_{IN} = 1\,\mathrm{mW}$, $BW = 1\,\mathrm{Hz}$, $S/N = 3$ and the detector characteristics described in the previous paragraphs. The plot is computed by considering the light modulation frequency to always be equal to the noise corner frequency, a condition obtained by tuning the bias voltage for each f_{AC}. The advantage of operating at high frequency is remarkable, with a difference of about a factor 20 between 1 kHz and 1 MHz. This improvement comes without any modification in the photonic chip architecture, highlighting the importance of performing a correct readout of the PbTe detector.

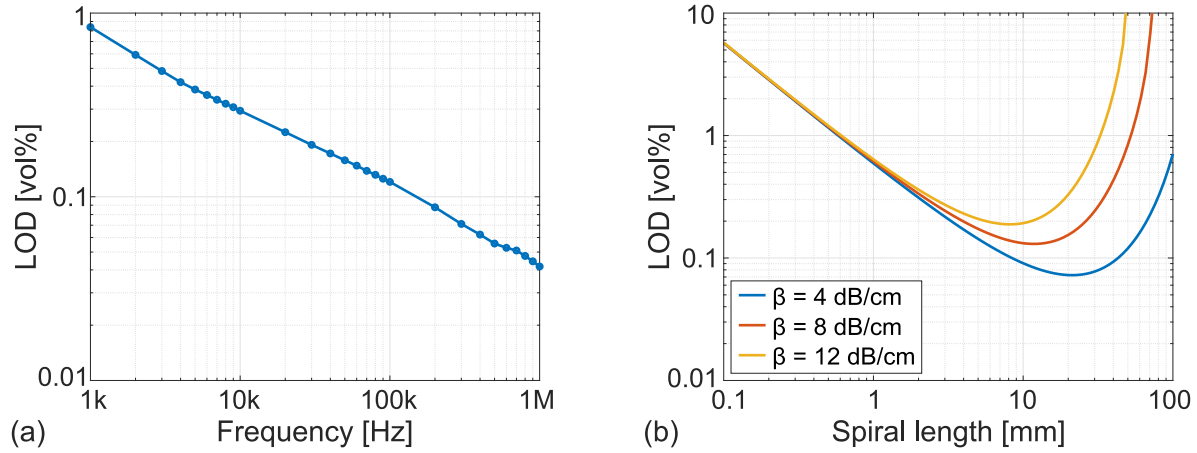

Fig. 8. (a) Theoretical LOD as a function of the light modulation frequency, computed by using the spiral parameters reported in [11] and the detector characteristics discussed in the previous paragraphs. (b) Theoretical LOD as a function of the sensing spiral length, calculated for different propagation losses of the chalcogenide waveguide and for $P_{IN} = 1\,\mathrm{mW}$, $f_{AC} = 1\,\mathrm{kHz}$.

Equation 7 also guides one through the design of the spiral sensing element. Both the propagation losses and the spiral length come into play in the calculation of the limit of detection. Lower waveguide losses allow one to use a long spiral without attenuating the light signal reaching the PbTe element, leading to higher power variations due to gas absorption. For the same reason, when waveguide losses are high a short spiral can be more effective than a long one, even if it has a reduced interaction length with gas. To quantify the effect of this trade-off, Figure 8b shows the LOD of the system as a function of the spiral length, for 3 values of propagation losses and $P_{IN} = 1\,\mathrm{mW}$, $f_{AC} = 1\,\mathrm{kHz}$. By properly sizing the spiral, a dramatic improvement in the measurement resolution can be obtained. Notice that the simulation is in good agreement with the experimental results reported in [12], where a LOD of 1% was obtained with a $5\,\mathrm{mm}$ long spiral. The small difference in the result can be attributed to the noise of the laser source, that is not considered in our simulation and was demonstrated to worsen the measurement resolution. The ultimate LOD limit can be reached by correctly sizing the spiral length to match the propagation loss and by operating at high frequency: in this condition, a LOD close to 0.001% is expected.

V. Conclusion

This work presented the complete characterization of a waveguide integrated PbTe detector for MIR applications. The measurement of the optical responsivity revealed the possibility of operating the detector over a wide range of frequencies, given the almost flat frequency response between $1\,\mathrm{kHz}$ and $1\,\mathrm{MHz}$. The noise spectrum of the detector was reported for the first time and highlighted the presence of an unexpected 1/f term, which dominates the thermal noise at low frequency or high bias voltage. This 1/f contribution can compromise the measurement resolution if not taken into account. The noise spectrum, together with the flat frequency response, suggests the use of the lock-in technique to optimize the readout strategy and operate above the 1/f corner frequency where the noise is minimum. As a practical example of the advantages obtained from a careful co-design of sensing element and readout electronics, the limit of detection of a gas sensing system based on PbTe detectors was investigated. The study revealed that optimized sensor system performance relies on an appropriate choice of parameters such as detector bias voltage, working frequency, and sensing spiral length. Optimization allows one to reduce the LOD from the current 1% down to 0.001%, a dramatic improvement that enables applications requiring high detection sensitivity/resolution. The future vision is a compact sensing system with very high resolution in the detection of target gases, liquids and aerosols, with applications in the fields of industrial and environmental pollution monitoring, food monitoring, medical diagnostics and drug delivery.

Acknowledgment

This work was partly supported by Progetto Rocca Foundation.

References

[1] M. Böberl, T. Fromherz, J. Roither, G. Pillwein, G. Springholz, and W. Heiss, "Room temperature operation of epitaxial lead-telluride detectors monolithically integrated on midinfrared filters," *Applied Physics Letters*, vol. 88, no. 4, pp. 1–3, 2006.

[2] T. H. Johnson, H. T. Cozine, and B. N. McLean, "Lead selenide detectors for ambient temperature operation," *Applied Optics*, vol. 4, no. 6, pp. 693–696, 1965.

[3] J. C. Slater, "Barrier theory of the photoconductivity of lead sulfide," *Physical Review*, vol. 103, no. 6, pp. 1631–1644, 1956.

[4] P. K. Basu, T. K. Chaudhuri, K. C. Nandi, R. S. Saraswat, and H. N. Acharya, "Preparation and characterization of chemically deposited lead sulphide thin films," *Journal of materials science*, vol. 25, no. 9, pp. 4014–4017, 1990.

[5] N. B. Kotadiya, A. J. Kothari, D. Tiwari, and T. K. Chaudhuri, "Photoconducting nanocrystalline lead sulphide thin films obtained by chemical bath deposition," *Applied Physics A*, vol. 108, no. 4, pp. 819–824, 2012.

[6] T. Safrani, T. A. Kumar, M. Klebanov, N. Arad-Vosk, R. Beach, A. Sa'ar, I. Abdulhalim, G. Sarusi, and Y. Golan, "Chemically deposited PbS thin film photoconducting layers for optically addressed spatial light modulators," *Journal of Materials Chemistry C*, vol. 2, no. 43, pp. 9132–9140, 2014.

[7] A. B. Rohom, P. U. Londhe, P. R. Jadhav, G. R. Bhand, and N. B. Chaure, "Studies on chemically synthesized PbS thin films for IR detector application," *Journal of Materials Science: Materials in Electronics*, vol. 28, no. 22, pp. 17 107–17 113, 2017.

[8] T. S. Moss, "Lead salt photoconductors," *Proceedings of the IRE*, vol. 43, no. 12, pp. 1869–1881, 1955.

[9] R. J. Cashman, "Film-type infrared photoconductors," *Proceedings of the IRE*, vol. 47, no. 9, pp. 1471–1475, 1959.

[10] F. S. Terra, M. Abdel-Rafea, and M. Monir, "Photoconductivity and electrical properties of $Pb_{1-x}Sn_xTe$ thin films," *Journal of Materials Science: Materials in Electronics*, vol. 12, no. 10, pp. 561–567, 2001.

[11] Z. Han, P. Lin, V. Singh, L. C. Kimerling, J. Hu, K. Richardson, A. M. Agarwal, and D. T. H. Tan, "On-chip mid-infrared gas detection using chalcogenide glass waveguide," *Applied Physics Letters*, vol. 108, no. 14, p. 141106, 2016.

[12] P. Su, Z. Han, D. Kita, P. Becla, H. Lin, S. Deckoff-Jones, K. Richardson, L. C. Kimerling, J. Hu, and A. Agarwal, "Monolithic on-chip mid-IR methane gas sensor with waveguide-integrated detector," *Applied Physics Letters*, vol. 114, no. 5, p. 051103, 2019.

[13] B. Tuzson, M. Graf, J. Ravelid, P. Scheidegger, A. Kupferschmid, H. Looser, R. P. Morales, and L. Emmenegger, "A compact QCL spectrometer for mobile, high-precision methane sensing aboard drones," *Atmospheric Measurement Techniques*, vol. 13, no. 9, pp. 4715–4726, 2020.

[14] Z. Han, V. Singh, D. Kita, C. Monmeyran, P. Becla, P. Su, J. Li, X. Huang, L. C. Kimerling, J. Hu, A. Agarwal *et al.*, "On-chip chalcogenide glass waveguide-integrated mid-infrared PbTe detectors," *Applied Physics Letters*, vol. 109, no. 7, p. 071111, 2016.

[15] J. Wang, J. Hu, X. Sun, A. M. Agarwal, L. C. Kimerling, D. R. Lim, and R. A. Synowicki, "Structural, electrical, and optical properties of thermally evaporated nanocrystalline PbTe films," *Journal of Applied Physics*, vol. 104, no. 5, p. 053707, 2008.

[16] L. Zhang, J. Ding, H. Zheng, S. An, H. Lin, B. Zheng, Q. Du, G. Yin, J. Michon, Y. Zhang *et al.*, "Ultra-thin high-efficiency mid-infrared transmissive huygens meta-optics," *Nature communications*, vol. 9, no. 1, pp. 1–9, 2018.

[17] J. O. Dimmock and G. B. Wright, "Band edge structure of PbS, PbSe, and PbTe," *Physical Review*, vol. 135, no. 3A, p. A821, 1964.

[18] A. Bafekry, C. Stampfl, and F. M. Peeters, "The electronic, optical, and thermoelectric properties of monolayer PbTe and the tunability of the electronic structure by external fields and defects," *Physica Status Solidi (b)*, vol. 257, no. 6, p. 2000182, 2020.

[19] K. Hummer, A. Grüneis, and G. Kresse, "Structural and electronic properties of lead chalcogenides from first principles," *Physical Review B*, vol. 75, no. 19, p. 195211, 2007.

[20] J. Wang, J. Hu, P. Becla, A. M. Agarwal, and L. C. Kimerling, "Room-temperature oxygen sensitization in highly textured, nanocrystalline PbTe films: A mechanistic study," *Journal of Applied Physics*, vol. 110, no. 8, p. 083719, 2011.

[21] F. N. Hooge, "1/f noise is no surface effect," *Physics Letters A*, vol. 29, no. 3, pp. 139–140, 1969.

[22] E. O. Wrasse, P. Venezuela, and R. J. Baierle, "Ab initio study of point defects in PbSe and PbTe: Bulk and nanowire," *Journal of Applied Physics*, vol. 116, no. 18, p. 183703, 2014.

[23] N. J. Parada and G. W. Pratt Jr, "New model for vacancy states in PbTe," *Physical Review Letters*, vol. 22, no. 5, p. 180, 1969.

[24] N. J. Parada, "Localized defects in PbTe," *Physical Review B*, vol. 3, no. 6, p. 2042, 1971.

[25] G. Gervasoni, M. Carminati, and G. Ferrari, "Switched ratiometric lock-in amplifier enabling sub-ppm measurements in a wide frequency range," *Review of Scientific Instruments*, vol. 88, no. 10, p. 104704, 2017.

[26] A. Schliesser, N. Picqué, and T. W. Hänsch, "Mid-infrared frequency combs," *Nature photonics*, vol. 6, no. 7, pp. 440–449, 2012.

[27] W.-C. Lai, S. Chakravarty, X. Wang, C. Lin, and R. T. Chen, "On-chip methane sensing by near-IR absorption signatures in a photonic crystal slot waveguide," *Optics letters*, vol. 36, no. 6, pp. 984–986, 2011.

[28] L. Tombez, E. J. Zhang, J. S. Orcutt, S. Kamlapurkar, and W. M. J. Green, "Methane absorption spectroscopy on a silicon photonic chip," *Optica*, vol. 4, no. 11, pp. 1322–1325, 2017.

[29] H. Lin, Z. Luo, T. Gu, L. C. Kimerling, K. Wada, A. Agarwal, J. Hu *et al.*, "Mid-infrared integrated photonics on silicon: a perspective," *Nanophotonics*, vol. 7, no. 2, pp. 393–420, 2018.

Emanuele Guglielmi was born in 1991. He received the bachelor's degree (cum laude), the master's degree in electronic engineering, and the Ph.D. degree (cum laude) in electronics from the Politecnico di Milano, Milan, Italy, in 2013, 2015, and 2019, respectively. In 2018, he spent six months at the Massachusetts Institute of Technology (MIT), Cambridge, MA, USA, to work on the subject of photonic–electronic integration. From 2019 to 2020, he worked as a Post-Doctoral Researcher at Politecnico di Milano. His main research topic was in the field of integrated photonics developing electronic control systems for complex photonics circuits. He is specialized in high-sensitivity measurements and in the design of custom low-noise readout electronics, having experience in developing discrete component boards (PCB) and CMOS-integrated circuits. He is currently CTO and co-founder of PhotonPath, an Italian startup and spin-off of Politecnico di Milano founded in 2019, that develops, manufactures and commercializes products based on integrated photonics for telecom, quantum and sensing applications.

Peter Su received a bachelor's degree from the University of Michigan - Ann Arbor in 2015 and a Ph.D. from the Massachusetts Institute of Technology (MIT) in 2020, both in Materials Science and Engineering. His research focused on materials and device designs for mid-infrared integrated photonic circuits.

Francesco Zanetto received the cum laude bachelor's, master's and PhD degrees in electronics engineering from Politecnico di Milano, Italy, in 2014, 2016 and 2021, respectively. He is now a Research Assistant with the Department of Electronics, Information and Bioengineering in the same university. He has been working on the development of low-noise analog and mixed-signal electronic circuits and instrumentation for photonic and nanoscience applications.

Katherine Stoll received bachelor's degrees in Materials Science & Engineering and Physics in 2019 at the Massachusetts Institute of Technology (MIT). She is currently a Materials Science and Engineering Ph.D. candidate at MIT and her research focuses on materials and structures for mid-infrared integrated photonics.

Samuel Serna received a double master's degree from the Friedrich-Schiller-University Jena, Germany, in photonics and the Institute d'Optique Graduate School Paris, France, in optics, matter and plasmas" (Erasmus Mundus Master scholarship: Optics in Science & Technology - OpSciTech), in 2013. He earned his PhD in 2016 at the University of Paris Sud in Science - Photonics and was postdoctoral researcher at the Centre for Nanoscience and Nanotechnology (C2N-Université Paris-Sud-Université Paris-Saclay). He was a postdoctoral associate at the Massachusetts Institute of Technology (MIT), where he is an invited professor. He is an assistant professor at Bridgewater State University (BSU) in Massachusetts since 2019.

Giorgio Ferrari (Member, IEEE) received the Laurea and Ph.D. degrees in electronics engineering from the Politecnico di Milano, Milan, Italy, in 1999 and 2003, respectively. Since 2005, he has been an Assistant Professor of electronics with Politecnico di Milano. The focus of his research activities is on the development of novel integrated instrumentation to probe electrical properties of materials and biosamples at the nanoscale. He has published more than 90 articles on international journals, nine book chapters, edited a book on capacitance spectroscopy of semiconductors, and holds nine patents.

Marco Sampietro (Member, IEEE) was born in 1957. He received the master's degree in nuclear engineering from the Politecnico di Milano, Milan, Italy, in 1982. From 2012 to 2018, he has been the Dean of the Bachelor and Master Course Program in Electronics Engineering at Politecnico di Milano, where he is currently a Full Professor of electronic circuits and devices. He is responsible for the activities in high-sensitivity instrumentation for the nanoscience, with a focus on the design of electronic integrated circuits for the measurement of currents, voltages, impedances, and noise to access the electronic properties of nano–bio-sensors. He has been a coordinator of many national and international research projects and a scientific partner in six large-size European projects. He is a coauthor of more than 200 peer-reviewed publications. He holds five patents.

Kazumi Wada is Professor Emeritus with The University of Tokyo, Bunkyo, Tokyo, Japan, and Research Scientist with the Department of Materials Science and Engineering, Massachusetts Institute of Technology, Cambridge, MA, USA. He is a Fellow and a recipient of the 11th Hayashi Izuo Award of Japan Society of Applied Physics.

Lionel C. Kimerling is the Thomas Lord Professor of Materials Science and Engineering at MIT and the Director of the MIT Microphotonics Center where he conducts an active research program in the design and processing of semiconductor materials and devices. He was Head, Materials Physics Research at AT&T Bell Laboratories when he joined the faculty of MIT as Professor. He was Director of the Materials Processing Center for 15 years, establishing it as the industry portal for faculty across all materials-related disciplines. He is the AIM Photonics Institute Executive for Education, Workforce Development and Technology Roadmap. He has authored more than 600 technical articles and more than 75 patents in the fields of integrated photonics and semiconductor processing. The Microphotonics Center Industry Consortium oversees more than 300 industrial, academic and government organizations that contribute to the Integrated Photonics System Roadmap, International (IPSR-I) releases. Kimerling was President, TMS; Chairman, Editorial Board of the Journal of Electronic Materials; and he has served on the Advisory Board, National Center for Photovoltaics, DOE and the National Materials Advisory Board, NRC. He is the recipient of the 1995 Electronics Division Award of the Electrochemical Society and the 1999 John Bardeen Award of TMS. He is a Fellow of the American Physical Society, the AAAS, TMS, MRS and the School of Engineering, UTokyo. His research teams have enabled long-lived telecommunications lasers, developed semiconductor diagnostic methods such as DLTS, SEM-EBIC and RF-PCD, and pioneered silicon microphotonics.

Anuradha Agarwal received the doctoral degree in electrical engineering from Boston University, Boston, MA, USA, in 1994, where she investigated the spatial extent of point defect interactions in silicon. She has been at Massachusetts Institute of Technology's Materials Research Laboratory since 1994, except for a short (2001–2004) stint at Clarendon Photonics, where she was a part of a team of engineers developing a novel optical filter. She is currently a Principal Research Scientist, and is developing integrated Si-CMOS compatible linear and nonlinear materials for photonic devices, especially in the mid-infrared regime, for hyperspectral imaging and chem-bio sensing because most chemical and biological toxins have their fingerprints in this range. She has more than 100 journal and refereed conference publications, 6 awarded patents, and 5 pending patents. Her work on mid-infrared materials and devices is creating a planar, integrated, Si-CMOS-compatible microphotonics platform which will enable on-chip imaging and sensing applications.